Under pressure: Syntectonic quartz veins in the Maverick Shale, Mazatzal Mountains, Arizona: Their timing, stress fields, and associated kinematic indicators

David Schneider
Department of Geology, Carleton College, One N. College St., Northfield, MN 55057
Faculty Sponsors: David Bice, Carleton College; Paul Karabinos, Williams College

INTRODUCTION

The central and northern portions of the N-S trending Mazatzal Mountains in central Arizona are characterized by fold and thrust fault geometries that resemble a classic foreland fold-and-thrust belt associated with thin-skinned tectonics (Doe and Karlstrom, 1991; Puls 1986). Dates obtained from pre-deformational and post-deformational granite intrusions constrain the age of the Mazatzal orogeny between 1690 Ma and 1650 Ma (Karlstrom and Bowring, 1991). The Mazatzal Orogeny is believed to be the last in a series of collisions that created the parallel mountain ranges in the Transition Zone of Arizona, forming eight tectonic blocks bounded by NE-striking shear zones (Bowring and Karlstrom, 1990). Tectonic models of the orogeny remain tenuous due to the isolation of the tectonic blocks and the relatively understudied nature of the thrust belts. In the northern Mazatzal Mountains, low-grade metasedimentary rocks of the Mazatzal Group affected by folding and thrusting during the Mazatzal orogeny are exposed. Minor secondary features in the rocks, especially crystal fiber quartz veins, give new insight into the stresses associated with this Proterozoic deformational event.

Goals and previous work. The goal of this project is to characterize the kinematic framework of the northern Mazatzal Mountains and to determine the stress fields responsible for the deformation. Previous authors have focused on regional mapping and the geometries of large-scale folds and thrusts. None of the authors have fully characterized the stress fields, though most have found the trend of the greatest principal stress or transport direction. The most extensive work was been done by Puls (1986) who did regional mapping and described a progressive deformation history. Horstman (1980) considered joint orientations, fold axes, and a few en-echelon veins. His model included two distinct episodes of deformation. This project uses crystal fiber quartz veins and, to a lesser extent, other minor structural features, to reconstruct stress fields. Another goal of this project is to determine which of the deformational models, if any, are more plausible based upon the new data presented here and their correlation with previous data. Finally, the correlation of the structural framework and deformation history in the Mazatzal Mountains to that in the Slate Creek Shear Zone (SCSZ) is considered. The SCSZ may be one of the block-bounding shear zones. Its role in the Mazatzal Orogeny deformation and its structural connection to the Mazatzal Mountains is not well understood (Wessels and Karlstrom, 1991). Martin Wong (this volume) conducted a similar project in the overlying red member of Mazatzal Peak Quartzite formation.

Geology of field area. The field work was concentrated in the Proterozoic Maverick Shale, a 115 m-200 m thick formation of interbedded quartzite and metapelite. Grain size ranges from clay to very coarse sand with some pebbles. The formation is greenish to gray siltstone to shale in its lower section, and tan to yellow siltstone, fine to coarse sandstone, and some shale in its upper portions. Interbedded 0.5-2 m thick beds of mature quartz arenite are frequently found in the upper section of the Maverick Shale. For more discussion on the sedimentology of the Maverick Shale, see Sammons, this volume. The most accessible and best exposures of the Maverick Shale are on the eastern side of the mountain range in Barnhardt and Shake Tree Canyons, where most of the data come from, although outcrops to the north near the Rock Creek Trail and around North Peak were also studied. The Maverick Shale in Barnhardt and Shake Tree Canyons is believed to be a zone associated with the Barnhardt thrust that accommodated a relatively high amount of motion (Doe and Karlstrom, 1991).

RESULTS

Veins. The majority of veins in the Maverick Shale are traceable for a meter or less and occur only in the more competent quartzite beds (Fig. 1a). They are typically 1-2 cm wide and spaced 50 cm or more apart. Out of 119 veins measured, the most significant vein cluster (93 veins) strikes NW-SE around 135° (315°) and dips to the SW at angles of 65° to nearly vertical. Fibers in the veins are nearly perpendicular to the walls of the vein (Fig. 1b). Under thin section, these veins have stretched quartz crystal fibers, marked by elongate "needles" that have high length to width ratios. The fibrous crystals in the veins are several times larger than in the parent rock, are nearly

optically continuous across the vein, and have a saw-tooth pattern between the grains. These features are among the characteristics of stretched crystal fiber veins described by Ramsay and Huber (1983) (Fig. 2a).

Cleavage. Slaty cleavage in the Maverick Shale is sporadically developed. The best development of cleavage is in the lowermost section of the formation in the clay-silt beds that are exposed in the main drainage of Barnhardt Canyon. In the upper section of the Maverick Shale, where incompetent beds are interbedded with quartzite layers, cleavage is found near the hingelines of folds. It forms an axial-planar cleavage (Fig. 2b).

Folds. The orientations of several tight, sub-horizontal, moderately inclined, asymmetric, chevron and circular folds of relatively small amplitude (≈1-2m) were measured in the upper part of the Maverick Shale in both Barnhardt and Shake Tree Canyons (Fig. 2c). The folds often involve layers of differing competence (quartzite and shale) and fit a flexural-slip folding model. Cleavage in the incompetent layers is a component of this model, as are the mullions that outcrop in a couple areas of the Maverick Shale. Mullions formed at the interface between the strong quartzite layers and weaker clay-silt layers.

Quartz Fiber Lineations. Quartz fiber lineations, developing slikensided surfaces, are found on bedding-parallel slip surfaces in the Maverick Shale (Fig. 2d). They constitute another component of the flexural-slip folding model.

Joints. Joint orientations were also measured in the Maverick Shale (Fig. 2e), but their genetic origin was difficult to interpret and the data were not used in the analysis discussed below. Although often a part of a flexural-slip folding model, the joints measured here did not show the geometry that is normally associated with cross-joints and longitudinal joints around fold axes (Ramsay and Huber, 1983).

DISCUSSION

The orientations of the greatest principal stress, σ_1, and the least principal stress, σ_3, were determined independently from different structures (Fig. 3). As noted above, the quartz veins in the Maverick Shale are of the stretched crystal fiber type described by Ramsay and Huber (1983). The temperature needed for their emplacement constrains them to low-grade syntectonic conditions. Fibers in this type of vein grow parallel to the direction of displacement, which corresponds to the orientation of σ_3. In this data set, since the fibers are perpendicular to the walls of the veins, the poles to the veins approximate the orientation of σ_3. Using Neil Mancktelow's application program Stereoplot, poles to the veins were plotted on an equal-area projection and contoured at 2% intervals. This allowed the preferred orientations of the poles to be seen and the implied orientation of σ_3 to be measured at the highest pole density.

Cleavage, fold axes, and quartz fiber lineations served as proxies for the orientation of σ_1, as their strain significance and implied stress orientations are fairly well understood. The methods used to find σ_1 from each structure were similar to those used for veins. An average value of σ_1 was then calculated from these three structures and it fell on the best-fit great circle (σ_1/σ_3 plane) that Stereoplot calculated for the poles of veins, crystal fiber lineations, poles to cleavage, and poles to fold axial planes. The values obtained for σ_1 and σ_3 are perpendicular lines, as they should be in theory. σ_2 was determined by finding the pole to the σ_1/σ_3 plane. It is unclear whether there is any structural feature that represents σ_2. The data are consistent with one episode of deformation, since the features do not imply any fundamental shifts in the stress fields. The thrusting orientation/σ_1 interpretation agrees with previous studies (Fig 4) and suggests that the kinematic framework has been adequately characterized.

The majority of veins represented in these data formed late relative to folding and thrusting. This conclusion is based on the fact that the veins are consistently oriented relative to one another and do not have a consistent orientation relative to bedding. If they had a consistent orientation relative to bedding, that would suggest that they had formed prior to folding and were then rotated. In addition, the veins do not have a typical geometric relationship to fold axes. They are neither parallel or perpendicular to fold axes, so their origin as cross joints or longitudinal joints can be ruled out. Fracture produced by increasing pore fluid pressure due to the overburden of thrusts may be an origin of the extensional veins. Although σ_3 may not have been extensional, pore fluid pressure could have instantaneously caused tensile fracture by decreasing hydrostatic stress. Fractures can create a place of low pressure to which fluids migrate, causing nucleation of quartz crystals that grow simultaneously with the fracture opening. The veins are mostly of the stretched fiber type and therefore are not useful as progressive strain indicators. Other structures, including folds, cleavage, mullions, and crystal fiber lineations are consistent with models of flexural slip folding, when mechanically stiff layers and mechanically weak layers alternate and have a strong influence on the deformation style.

The data are consistent with Puls' (1986) proposed sequence of a single progressive deformation episode which is a typical model for fold and thrust belts. The origin of the relatively late veins can be added to this model. Adapting Puls's sequence of events, first initial SE/NW compression produced layer parallel shortening of the

Mazatzal Group rocks (Deadman Quartzite, Maverick Shale, and Mazatzal Peak Quartzite), leading to buckling of the layers and cleavage formation in the Maverick Shale. Second, layer parallel shear occurring with early thrusting resulted in large tight, asymmetric folds. Next, thrusting thickened the Mazatzal Group rocks and truncated folds. Next, Puls's model includes continued thrusting, development of duplex structures, fault propagation folds, and rotation of some of the earlier folds. At this point, vein development could occur at depth due to the increase in pore fluid pressure caused by the overburden of thrust sheet emplacement. The section was then transported over the underlying Alder Group Rocks by thrust faults at depth.

Wessels and Karlstrom (1991) propose that this deformation in the Mazatzal Mountains was concurrent with deformation in the SCSZ, but that deformation in the SCSZ outlasted that in the Mazatzal Mountains. The kinematic framework in the mountains and the shear zone is similar, yet σ_1 in the SCSZ is oriented more to the north than that in the mountains. Wessels and Karlstrom propose that the fabric in the SCSZ may have been rotated towards the NW. The data presented here are consistent with that model, yet much more work could be done in describing the stress fields in the SCSZ and correlating the progressive strain histories in the SCSZ with the Mazatzal Mountains.

REFERENCES

Alvis, M.R., 1984, Metamorphic petrology, structural and economic geology of a portion of the central and northern Mazatzal Mountains, Gila and Maricopa counties, Arizona [M.S. thesis]: Northern Arizona University, 129p.

Bowring, S.A., and Karlstrom, K.E., 1990, Growth, stabilization, and reactivation of Proterozoic lithosphere in the southwestern United States: Geology, v. 18, p. 1203-1206.

Doe, M.F., and Karlstrom, K.E., 1991, Structural Geology of an Early Proterozoic Foreland Thrust Belt, Mazatzal Mountains, Arizona: Arizona Geological Society Digest, v. 19, p. 181-192.

Horstman, K.C., 1980, Geology of the Club Ranch Area, Mazatzal Mountains, Arizona [M.S. thesis]: Flagstaff, Northern Arizona University, 71 p.

Karlstrom, K.E. and Bowring, S.A, 1991, Styles and timing of Early Proterozoic deformation in Arizona: Constraints on Tectonic models: Arizona Geological Society Digest, v. 19, p. 1-10.

Puls, D.D., 1986, Geometric and Kinematic analysis of a Proterozoic foreland thrust belt, northern Mazatzal mountains, central Arizona [M.S. thesis]: Flagstaff, Northern Arizona University, 102p.

Ramsay, J.G., and Huber, M.I., 1983, The Techniques of Modern Structural Geology, vol. 1, Strain Analysis. New York: Academic Press.

Wessels, R.L., and Karlstrom, K.E., 1991, Evaluation of the Significance of the Proterozoic Slate Creek Shear Zone in the Tonto Basin Area: Arizona Geological Society Digest , v. 19, p. 193-209.

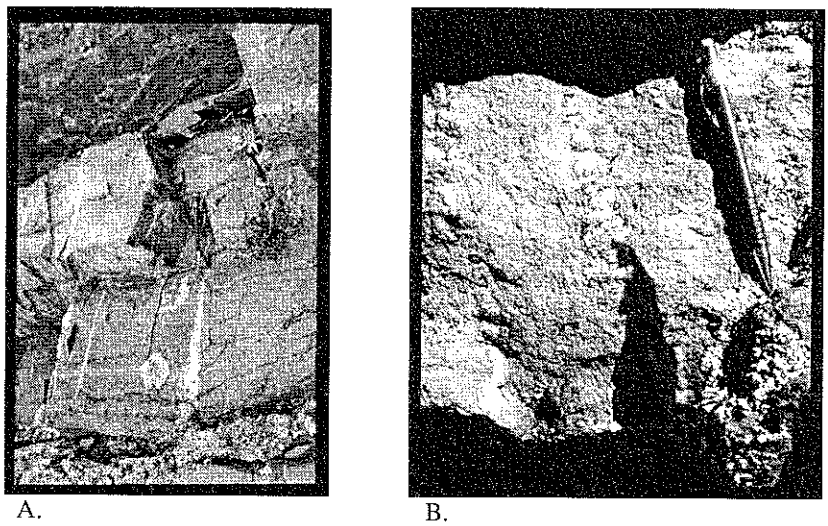

A. B.

Figure 1. (a) Typical quartzite outcrop in the Maverick Shale with preserved bedding features and fibrous quartz veins. Pencil for scale, length is about 15 cm. (b) Fibrous quartz vein with wall perpendicular fibers, center of picture. Same pencil for scale.

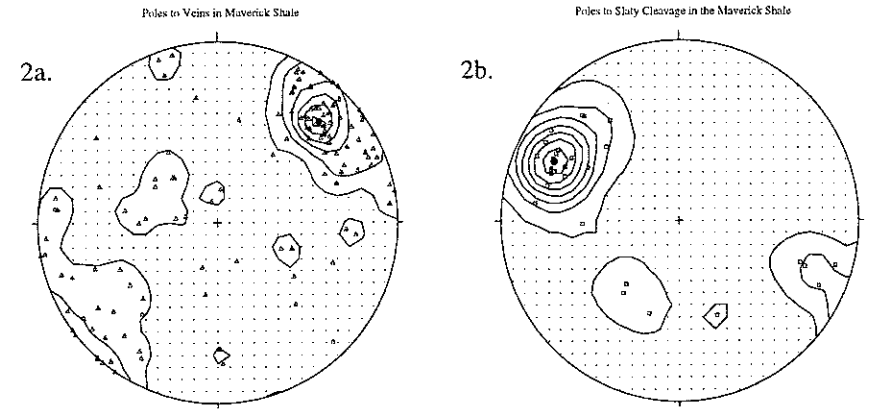

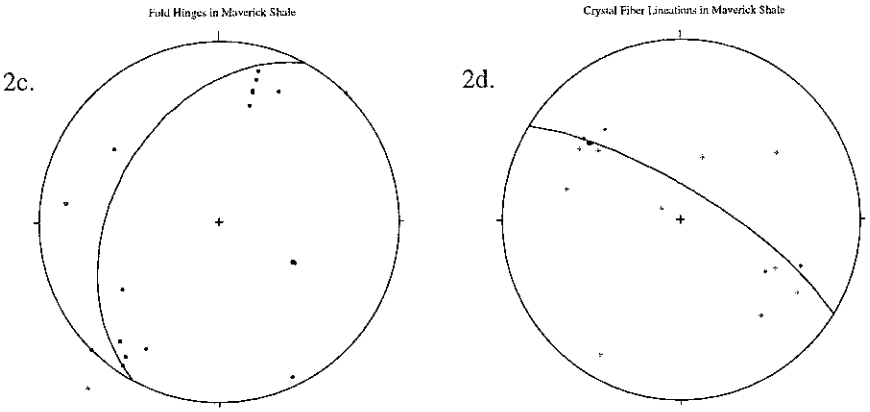

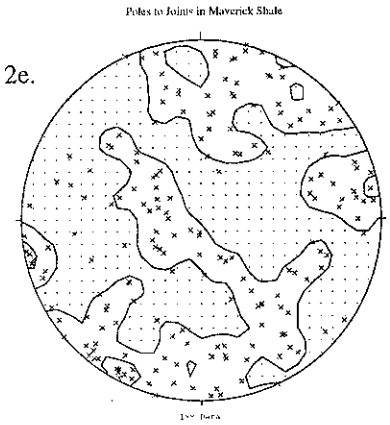

Figure 2. All plots are equal- area plots of structural features in the Maverick Shale, contoured at 2% intervals where appropriate. (a) Poles to veins (△), with a dominant cluster in the NE quadrant. (b) Poles to slaty cleavage (□), with apparent NW cluster. (c) Poles to fold axes (◇), with best-fit great circle representing the axial plane. (d) Orientation of crystal fiber lineations (+). (e) Poles to joints (x), showing a scattered distribution.

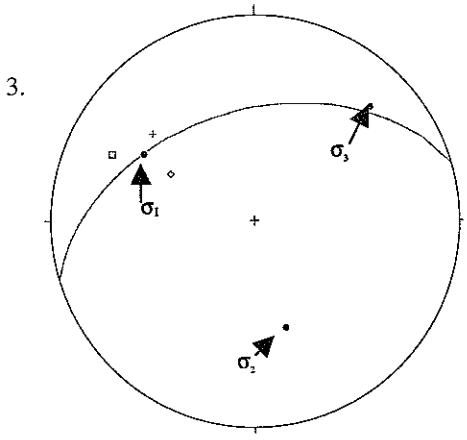

△ Veins □ Cleavage
+Crystal fibers ◇ Folds
• Principal Stress Directions

Figure 3. Interpreted principal stress directions, represented as large dots. Orientations (trend (T) and plunge (P) are:
σ_1 = T 301°, P 36°
σ_2 = T 164°, P 45°
σ_3 = T 46°, P 22°.

Author and structural evidence	Interpretation of σ_1/thrusting direction
Puls (1986). Used folds, cleavage, faults, crystal fibers.	Trend 310°
Alvis (1984). Used cleavage.	Trend 304°
Horstman (1980). Used joints, c-axes, folds, veins.	First, N-S trend; second trend 296°
Doe and Karlstrom (1991). Used crystal fiber lineations.	Trend 289°

Figure 4. Analysis of structures in the Mazatzal Mountains by other authors found these results for the trend of the greatest principal stress. The results compare favorably to mine, with the exception that Horstman (1980) believed that there were two episodes of deformation.